Cyber-physical-transportation System based Co-design of Charging Pricing and Frequency Regulation Control for EVs in Multi-market

Lei Xu, Chunxia Dou, *Fellow*, *IEEE*, Dong Yue, *Fellow*, *IEEE*, Houjun Li, and Yanlin Ji

***Abstract*—With the gradual integration of vehicle-to-grid technology in electric vehicles (EVs), the interaction between transportation and distribution networks has become increasingly critical, intensifying the demand for power grid communication and transforming the power grid into a cyber-physical-transportation system. In response to these challenges, this paper proposes a pricing and control strategy for battery changing stations (BCSs) across multiple markets. Firstly, a Bayesian adaptive spline surface based sensitivity analysis method is employed to quantify the impact of pricing on road congestion rates. In the intraday market, a dynamic pricing strategy, guided by sensitivity analysis, is designed to influence EV traffic flow with minimal price adjustments. This optimizes BCS revenue in energy and reserve capacity markets while alleviating traffic congestion and reducing the communication burden. In the real-time market, a game-based subjective and objective evaluation method is developed to assess the response characteristics of BCSs considering factors such as communication delays, regulation capacity, and market revenue, enabling an equitable allocation of frequency regulation tasks among BCSs. Additionally, this method ensures fair compensation to balance the financial impact of price changes across multiple BCSs. Simulation results validate the effectiveness of the proposed method.**

***Index Terms*—Charging pricing, cyber-physical-transportation system, electric vehicle, frequency regulation, multi-market interaction.**

I. Introduction

With the growing popularity of electric vehicles (EVs) and vehicle-to-grid (V2G) technology, battery charging stations (BCSs) have become a critical interaction point between EVs and power grids. However, large-scale integration of EVs poses new challenges to grid stability, particularly in terms of supply-demand balance and grid frequency stability [1], [2]. Furthermore, the demand for informatization continues to rise, the coupling of EVs, information networks, distribution networks (DN), and transportation networks (TN) forms a typical cyber-physical-transportation system (CPTS) [3]. In addition, within a complex market environment, factors such as fluctuating charging prices and varied demand for EV charging make multi-level coordination within the CPTS increasingly intricate [4]. Consequently, research is increasingly focused on the development of pricing and control methods for BCSs within the CPTS framework.

BCS pricing methods are explored with consideration of the coupling between DN and TN. Reference [5] develops a game-based model to capture the complex interplay between a profit-maximizing generator and a utility-maximizing EV driver. Reference [6] leverages the energy storage capabilities and spatio-temporal distribution characteristics of EVs to mitigate fluctuating electricity prices and minimize costs. However, these researches employ the user equilibrium (UE) model to simulate traffic flows, which is constructed based on the individual rationality of EVs [7], [8], while ignoring the impact of traffic congestion and focusing solely on operational costs for economic optimization. In contrast, the social optimal (SO) model aims to maximize social welfare and has been used to propose congestion pricing method to alleviate urban traffic congestion [9]. Reference [10] proposes congestion pricing through independent transport system operators, whereas reference [11] suggests optimal congestion prices based on intraday dynamics of transportation and power flow. However, they are designed from the perspective of transportation authorities, placing the cost burden on EV users while primarily benefiting regulatory parties, thus posing challenges to implementation. Moreover, the TN optimization targeted by [5], [6],

Received: November 20, 2024
Accepted: September 1, 2025
Published Online: November 1, 2025
Lei Xu, Chunxia Dou (corresponding author), Dong Yue (corresponding author), and Houjun Li are with the Institute of Advanced Technology for Carbon Neutrality, Nanjing University of Posts and Telecommunications, Nanjing 210000, China (e-mail: xulei_688@163.com; cxdou@ysu.edu.cn; medongyue@vip.163.com; lihoujunertou@163.com).
Yanlin Ji is with the School of Engineering and Informatics, University of Sussex, Brighton BN1 9RH, UK (e-mail: yj236@sussex.ac.uk).
DOI: 10.23919/PCMP.2024.000403

[10]–[12] is often in a stable state and less effective for addressing ongoing congestion issues. Regarding the coupling between BCSs and communication networks, reference [13] proposes an event-triggered method to mitigate the delay in EV frequency regulation (FR) control. Reference [14] introduces a resource efficiency method to balance spectrum efficiency and cost in V2G communication networks, and reference [15] develops a combined optimization method for dynamic spectrum allocation and EV scheduling in virtual power plants. However, these methods are not integrated into the pricing process. A rational pricing mechanism can guide traffic allocation to align with communication burden distribution, thereby improving communication efficiency, reducing energy consumption, and ensuring low-latency communication.

The correlation between road congestion rates and BCS prices presents critical implications for system optimization. While data-driven methods, including support vector regression (SVR) [16], random forest algorithm [17], and neural networks [18], are widely adopted for their predictive capabilities, their inherent "black-box" nature limits interpretability when quantifying variable relationships. To address this limitation, Sobol's sensitivity analysis theory, grounded in variance decomposition [19], offers a robust framework for evaluating the relative importance of input variables. By decomposing model output uncertainty into contributions from individual inputs, this method enhances the interpretability of the model. The Monte Carlo sampling method, commonly employed for calculating Sobol indices, faces significant computational challenges due to the requirement for extensive iterative sampling [20], [21]. To alleviate this bottleneck, this paper proposes to construct a computationally efficient meta-model for sampling simulations. By repeatedly executing the meta-model to derive Sobol sensitivity indices, the computational burden is alleviated. Specifically, Bayesian adaptive spline surfaces (BASS) is selected as the meta-modeling framework for its dual advantages: 1) the ability to incorporate prior domain knowledge with observed data [22]; and 2) the ability to generate probabilistic interpretations of results through posterior distributions [23].

Numerous researches have been conducted to optimize the interaction between BCSs and the DN. Some focus on maximizing BCS revenue by integrating EV participation in market clearing with renewable energy sources [24], incorporating TN models into market bidding [25], and applying conditional value at risk (CVaR) to mitigate market price volatility [26]. However, these researches overlook potential revenue opportunities from reserve capacity (RC) markets and FR [27]. Reference [28] proposes a joint economic dispatch and FR service model for EVs that facilitated by an EV aggregator, while reference [29] presents a two-stage optimization algorithm for EV aggregation and charging power management, balancing FR revenue with charging cost. Additionally, reference [30] accounts for energy and FR price uncertainties in EV charging schedules but does not incorporate RC markets into its pricing mechanisms.

Most existing research prioritizes day-ahead market economic optimization of BCSs, neglecting benefit equilibrium among them in the real-time market. Regarding real-time EV control strategies, several researches have proposed optimal dispatch models aimed at minimizing operational costs [31]. However, they ignore the dynamic response characteristics of EVs, such as FR capacity (FRC) [32], [33], and battery state of charge (SOC) [34], [35]. These characteristics have been independently adopted as FR task allocation, but the single-factor evaluation frameworks inherently lack comprehensive consideration. Reference [28] suggests combining SOC and FRC as allocation indices, while reference [36] develops mixed-integer linear programming (MILP) models incorporating multiple factors. However, these models typically apply equal weights to different parameters, which may cause bias on the EV side. To address this limitation, reference [37] proposes a power allocation method based on the analytical hierarchy process (AHP) that considers the relative importance of cost, power system contingency, and load balancing. However, AHP relies on subjective judgment and lacks quantitative objectivity [38]. Subsequent studies attempt to improve this through fuzzy logic extensions [39] or hybrid evaluation frameworks [40], but these methods still maintain equal weighting between subjective and objective factors, leading to potential inaccuracies in multi-microgrid and photovoltaic hybrid systems. To overcome this limitation, this paper proposes a game based subjective and objective evaluation method, using fuzzy analytic hierarchy process (FAHP) and criteria importance through intercriteria correlation (CRITIC) methods to evaluate the FR characteristics of BCS.

The main contributions of the paper can be summarized as follows.

1) This paper proposes a novel pricing mechanism from the EV aggregator (EVA) perspective, incorporating economic incentives derived from traffic congestion mitigation. The framework establishes an equilibrium between regulatory objectives and EV user interests, significantly improving the feasibility and practicality of the method implementation.

2) A BASS-based sensitivity analysis quantifies the coupling relationship between charging prices and road congestion rates. Then, a sensitivity-based dynamic pricing method is proposed to guide the flow of EVs through minimal charging price adjustments, simultaneously balancing communication resource allocation and congestion alleviation.

3) An intraday pricing method is proposed to achieve the co-optimization of energy and RC market. Specifically, this method considers the joint optimization of the purchase price, charging price, and FRC schedule,

aiming to maximize the economic benefits of BCS through multi-market interaction.

4) In the real-time market of EV control, this paper proposes a hybrid FR response capability evaluation method. This integrates game-based FAHP evaluation and CRITIC evaluation method, which improves the accuracy of evaluation and effectively avoids problems such as power overrun and BCS income imbalance caused by the conventional equal-weight method.

The rest of this paper is organized as follows. In Section II, the proposed system is described in detail. Section III presents the sensitivity analysis of BCS charging prices to road congestion, while Section IV focuses on charging pricing and scheduling of BCSs in the intraday market. Furthermore, Section V discusses FR control of BCSs in the real-time market. Section VI provides the simulation results. Finally, Section VII summarizes this paper.

II. System Description

This paper proposes a BCS pricing and control method to determine the optimal charging price, schedule, and FR tasks in the CPTS. As shown in Fig. 1, the CPTS architecture comprises three hierarchical layers. The EVA controller interacts with distributed BCSs positioned across TN nodes. Radiating communication links establish interconnections between the aggregation controller and BCSs. Figure 2 illustrates the integrated pricing and control architecture of BCSs, demonstrating bidirectional interactions with both TN and DN. The communication system plays a crucial role in the V2G process, enabling BCSs to maintain seamless interaction with the power grid and operate as an integrated system. Through embedded communication modules, BCSs are able to comprehensively gather EV state information, such as real-time charging status and user-specified charging objectives. These data are transmitted through communication channels, ensuring real-time accuracy and reliability.

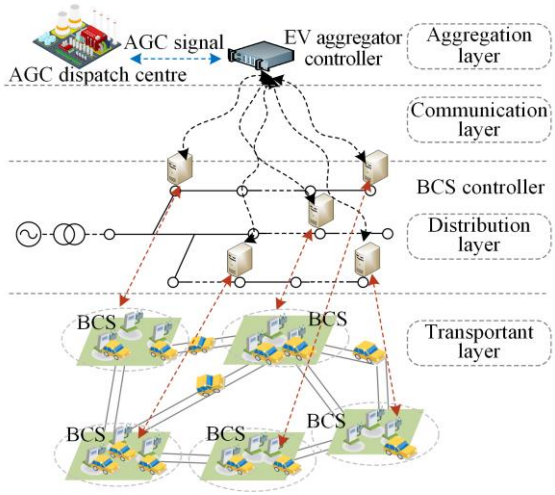

Fig. 1. CPTS framework of EVs.

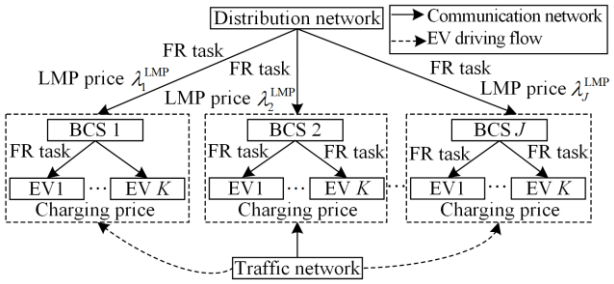

Fig. 2. Control framework of EVA.

Notably, this paper reformulates the problem of congestion pricing from the perspective of EV users and the issue of economic profit from the government's perspective into a pricing-guided traffic relief and economic subsidy framework from the perspective of the EVA. Specifically, EVA adjusts charging price to mitigate traffic congestion while capturing economic subsidies. EVA aims to minimize the cost of power purchases and maximize the benefit by providing FRC. Subsequently, BCSs respond to automatic generation control (AGC) signals from the DN to participate in frequency regulation.

III. Sensitivity Analysis of BCS Charging Price to Road Congestion

In this section, the BASS model in combination with the Sobol method, is employed to analyze the sensitivity of BCS pricing to road congestion based on the UE model.

A. TN Model

The UE model allocates EV travel demand between origin-destination (O-D) pairs to individual roads, determining the flow distribution across the network. In this paper, road congestion is represented by travel flow. According to the Bureau of Public Roads (BPR), the road congestion rate is defined as follows [41]:

$$R_a = x_a / x_a^{\text{base}} \text{ or } R_j = x_j / x_j^{\text{base}} \tag{1}$$

$$\left(\{x_a\},\{x_j\}\right) = \text{UE}(\lambda_{j,t}^{\text{C}}) \tag{2}$$

where R_a and R_j are the congestion rate in the ath road flow and jth BCS charging flow; x_a and x_j are the corresponding road flow and charging flow; x_a^{base} and x_j^{base} are the corresponding base value of road flow and charging flow; and $\text{UE}(\cdot)$ is the nonlinear user equilibrium model that establishes a mapping relationship between BCS charging prices and traffic flow [41].

B. BASS-based Sensitivity Analysis of BCS Charging Price to Road Congestion

The BASS-based meta-model is formulated as:

$$y_b = f(x_b) + \epsilon_b, \quad \epsilon_b \sim N(0, \sigma^2) \tag{3}$$

where y_b represents the bth output variables; x_b represents the bth input variables; ϵ_b is a residual that

follows a normal distribution with a mean of zero and a standard deviation of σ; and the function $f(\cdot)$ can be expressed as a basis function, which is a tensor product of segmented polynomials of order.

$$f(x)=h_0+\sum_{m=1}^{M}h_m\prod_{k=1}^{K_m}g_{k,m}\left[s_{k,m}(x_{k,m}-t_{k,m})\right]_+^h \quad (4)$$

where $h=(h_0,\ h_1,\ \cdots,\ h_m,\ \cdots,\ h_M)$ is the basis function coefficients and h_m is the the coefficient of the mth submodel; M is the number of basic functions; K_m is the mth maximum degree of interaction; $g_{k,m}$ is a constant for making the basis function with the maximum of one with the kth factor; $s_{k,m}$ is a sign indicator controlling the direction of the interaction; $t_{k,m}$ is a knot defining the location of the piecewise spline; and $[\cdot]_+^h$ is the function $\left(\max(0,\ \cdot)\right)^h$.

By analyzing the variance of each input and its interactions, the model output can be decomposed into its corresponding input. The specific steps of the Sobol sensitivity analysis are as follows.

Step 1: Obtain basic information about TN and DN, and select charging prices and traffic flow factors as system input variables $(\xi_b,\ \lambda_b)$.

Step 2: Using the UE model and statistical data, establish a coupled stochastic model that captures the relationship between traffic congestion rates and BCS charging prices.

Step 3: Generate input variable $(\xi_b,\ \lambda_b)$ through Sobol sequence sampling.

Step 4: Using the UE model, compute the corresponding output variables $Y=f(X_b,\ \xi_b,\ \lambda_b)$ of the TN for each set of sampled input variables.

Step 5: Set the sample size of the output variables and establish a transformation relationship between the input variables $(\xi_b,\ \lambda_b)$ and standard normal variables Z_b through the cumulative distribution function.

Step 6: Construct a BASS-based meta-model using standard normal samples Z_b as inputs and benchmark values as output samples $Y=f(X_b,\ \xi_b,\ \lambda_b)$.

Step 7: Calculate the global sensitivity $S_b^{'}$ of the BASS-based meta-model as:

$$S_b^{'}=\sum_{b\in A_u}a_b^2\Big/\sum_{b\in A_s}a_b^2 \quad (5)$$

where a_b represents the coefficient corresponding to orthogonal polynomial basis functions; A_s represents the set of indexes vectors corresponding to the key orthogonal polynomial basis functions; and A_u represents the set of positive vectors of A_s.

IV. Charging Pricing and Scheduling of BCSs in the Intraday Market

Figure 3 depicts optimization across multiple markets. BCS determines charging prices and schedules via the pricing and clearing in the intraday market, as detailed in Section IV.A and Section IV.B, respectively.

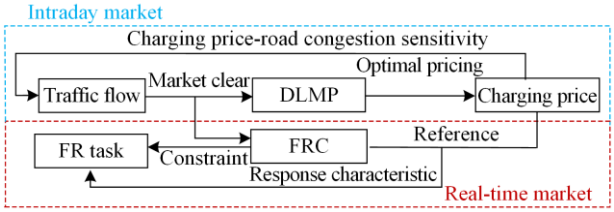

Fig. 3. Flowchart of BCS pricing and control.

A. The Market Clearing of EVA

With forecasted future loads and BCS charging loads, EVA optimizes the BCSs' charging schedules to minimize the power purchase cost in the energy market and maximize the benefits from FRC in the RC market. The optimization objective is described as:

$$J^{\mathrm{MC}}=\lambda_t^{\mathrm{LMP}}\sum_{j\in\pi(0)}(P_{0j,t}^{\mathrm{l}}-P_{j,t}^{\mathrm{RU}}\pi_{j,t}^{\mathrm{RU}}-P_{j,t}^{\mathrm{RD}}\pi_{j,t}^{\mathrm{RD}}) \quad (6)$$

$$\text{s.t.}\begin{cases}
P_{ij,t}+P_{j,t}^{\mathrm{g}}-r_{ij,t}l_{ij,t}=\sum_{k\in\pi(j)}P_{jk,t}+P_{j,t}^{\mathrm{c}}+P_{j,t}^{\mathrm{L}},\ \ \forall l\in E^{\mathrm{L}}\\
Q_{ij,t}+Q_{j,t}^{\mathrm{g}}-x_{ij,t}l_{ij,t}=\sum_{k\in\pi(j)}Q_{jk,t}+Q_{j,t}^{\mathrm{L}},\ \ \forall l\in E^{\mathrm{L}}\\
U_{j,t}=U_{i,t}-2(r_{ij,t}P_{ij,t}+x_{ij,t}Q_{ij,t})+(z_{ij,t})^2i_{ij,t},\ \ \forall l\in E^{\mathrm{L}}\\
i_{ij,t}U_{i,t}\geqslant(P_{ij,t})^2+(Q_{ij,t})^2,\ \ \forall l\in E^{\mathrm{L}}\\
P_{ij,t}\geqslant 0,\ \ \forall l\in E^{\mathrm{L}}\\
0\leqslant i_{ij,t}\leqslant i_{l,t},\ \ \forall l\in E^{\mathrm{L}}\\
U_{j,t}^{\min}\leqslant U_{j,t}\leqslant U_{j,t}^{\max},\ \ \forall j\in E^{\mathrm{N}}\\
P_{j,t}^{\min}\leqslant P_{j,t}^{\mathrm{g}}\leqslant P_{j,t}^{\max},\ \ \forall j\in E^{\mathrm{N}}\\
Q_{j,t}^{\min}\leqslant Q_{j,t}^{\mathrm{g}}\leqslant Q_{j,t}^{\max},\ \ \forall j\in E^{\mathrm{N}}\\
P_{j,t}^{\mathrm{c}}+P_{j,t}^{\mathrm{RD}}\leqslant P_{j,t}^{\mathrm{max,ch}}\\
P_{j,t}^{\mathrm{c}}-P_{j,t}^{\mathrm{RU}}(t)\geqslant -P_{j,t}^{\mathrm{max,dis}}\\
0\leqslant P_{j,t}^{\mathrm{c}}\leqslant P_{j,t}^{\mathrm{max,ch}}\\
S_{j,t}+\dfrac{P_{j,t}^{\mathrm{c}}+P_{j,t}^{\mathrm{f}}}{C_{j,t}^{\mathrm{battery}}}=S_{j,t+1}\\
0\leqslant S_{j,t}(t)\leqslant 1\\
S_{j,t}^{\mathrm{leave}}\geqslant S_{j,t}^{\mathrm{exp}}
\end{cases} \quad (7)$$

where i, j, k denote the upstream, current, and downstream nodes in the distribution network, respectively; λ_t^{LMP} is the purchase power price from upper power grid; $\pi(j)$ is the set of adjacent nodes of node j; $P_{0j,t}^{\mathrm{l}}$ is the active power flow of line j; $P_{j,t}^{\mathrm{RU}}$ and $P_{j,t}^{\mathrm{RD}}$ are the FRC for up regulation and down regulation, respectively;

$\pi_{j,t}^{\mathrm{RU}}$ and $\pi_{j,t}^{\mathrm{RD}}$ are the unit price of the FRC for up regulation and down regulation, respectively; E^{N} and E^{L} are the sets of lines and buses, respectively; $P_{ij,t}$ and $Q_{ij,t}$ are the active and reactive power of line between bus i and j, respectively; $P_{j,t}^{\mathrm{g}}$ and $Q_{j,t}^{\mathrm{g}}$ are the active and reactive power generated at bus j, respectively; $P_{j,t}^{\mathrm{c}}$ is the charging power at bus j, respectively; $P_{j,t}^{\mathrm{L}}$ and $Q_{j,t}^{\mathrm{L}}$ are the active and reactive power generated at bus j, respectively; $r_{ij,t}$, $x_{ij,l}$, and $z_{ij,l}$ are the line resistance, reactance, and impedance parameters, respectively; $l_{ij,t}$ is the squared line current; $U_{i,t}$ is the voltage magnitude of bus i; $i_{ij,t}$ and $U_{j,t}$ are the current and voltage magnitude of bus j, respectively; $i_{l,t}$ is the maximum current values; $U_{j,t}^{\min}$ and $U_{j,t}^{\max}$ are minimum and maximum voltage values, respectively; $P_{j,t}^{\min}$ and $P_{j,t}^{\max}$ are minimum and maximum values of active power, respectively; $Q_{j,t}^{\min}$ and $Q_{j,t}^{\max}$ are minimum and maximum values of reactive power, respectively; $P_{j,t}^{\mathrm{c}}$ is the charging power of BCS j; $P_{j,t}^{\max,\mathrm{ch}}$ and $P_{j,t}^{\max,\mathrm{dis}}$ are the maximum of BCS charging power and discharging power, respectively; $C_{j,t}^{\mathrm{battery}}$ is the aggregated battery capacity of BCS j; $S_{j,t}$ and $S_{j,t}^{\mathrm{leave}}$ are the aggregated SOC of BCS j at now and when leave, respectively; and $S_{j,t}^{\mathrm{exp}}$ is the aggregated expected SOC of BCS j.

B. The Optimal Pricing of BCSs

The pricing objectives include four parts: f_1 is for maximizing the profit from EV charging; f_2 is for maximizing the economic subsidy of traffic congestion relief; f_3 is for alleviating traffic congestion with minimum price change; and f_4 is for minimizing the communication burden for V2G. Therefore, the optimization objective can be expressed as:

$$F = \min(-f_1 - f_2 + f_3 + f_4) \tag{8}$$

$$\begin{cases} f_1 = \sum_{j\in J}\sum_{t\in T}(\lambda_{j,t}^{\mathrm{C}} - \lambda_{j,t}^{\mathrm{LMP}})P_{j,t}^{\mathrm{c}} \\ f_2 = \sum_{a\in\mathcal{N}}\left\|g_{a,t}x_{a,t}\right\|^2 \\ f_3 = \sum_{a\in\mathcal{N}}H_{a,t}\left\|\Delta F_{a,t}\right\|^2 \\ f_4 = \sum_{j\in J}\left\|x_j(\gamma_1\Delta D_j^{\mathrm{trans}} + \gamma_2\Delta E_j^{\mathrm{trans}})\right\|^2 \end{cases} \tag{9}$$

$$\text{s.t.}\begin{cases} \frac{1}{J}\sum_{j\in J}\lambda_{j,t}^{\mathrm{C}} = C_t^{'} \\ C_t^{'} > \lambda_t^{\mathrm{LMP}} \\ \lambda_{j,t}^{\mathrm{C,min}} \leqslant \lambda_{j,t}^{\mathrm{C}} \leqslant \lambda_{j,t}^{\mathrm{C,max}} \\ \Delta F_{a,t} = F_{a,t} - F_{a,t}^{\max} \\ F_{a,t} = S_{a,t}^{'}\lambda_{a,t}^{C} \\ g_{a,t} = \phi t_{a,t}^{0}\left(\frac{x_{a,t}}{C_{a,t}}\right)^{\gamma} \\ \Delta D_j^{\mathrm{trans}} = D_j^{\mathrm{trans}} - \bar{D}_j^{\mathrm{trans}} \\ \Delta E_j^{\mathrm{trans}} = E_j^{\mathrm{trans}} - \bar{E}_j^{\mathrm{trans}} \end{cases} \tag{10}$$

where J is the total amount of BCSs; T is the optimize cycle; $\mathcal{N}$ is the total amount of roads; $C_t^{'}$ is the average charging price level and is greater than the average power purchase price, which is used to ensure the profitability of BCSs; $\lambda_{j,t}^{\mathrm{C}}$ is the charging price at station j at time t; $\lambda_{j,t}^{\mathrm{LMP}}$ is the given electricity purchase price at station j, which can be obtained from the dual variables (shadow prices) associated with the bus power-balance constraints; $\lambda_{j,t}^{\mathrm{C,min}}$ and $\lambda_{j,t}^{\mathrm{C,max}}$ are the minimum and maximum charging prices at time t, respectively; $g_{a,t}$ is the congestion impedance/cost coefficient; $x_{a,t}$ is the traffic flow/usage of road cell a at time t; $\Delta F_{a,t}$ denotes the congestion rate deviation and is calculated by the sensitivity of the traffic congestion rate to the variation in charging prices; $F_{a,t}$ and $F_a^{\max}$ are the estimated value and up limit of traffic congestion on the ath road, respectively, which is settled by government departments; $S_{a,t}^{'}$ is the sensitivity of the traffic congestion rate to the charging prices; $H_{a,t} \in \{0, 1\}$ is a binary function that determine whether it is in a congested state, if $F_{a,t} > F_a^{\max}$, $H_{a,t} = 0$, otherwise $H_{a,t} = 1$; ϕ and γ are the blocking coefficients, usually taken as 0.15 and 4, respectively; $t_{aj,t}^{0}$ is the baseline travel time from road segment a to node j; $C_{a,t}$ is the saturation capacity of road unit; $\Delta D_j^{\mathrm{trans}}$ and $\Delta E_j^{\mathrm{trans}}$ are the bias transmitted data amount and energy consumption of the charging node, respectively; γ_1 and γ_2 are the weights applied to these two deviations in the objective; x_j is the station scale/weight used in f_4; D_j^{trans} and E_j^{trans} are the transmitted data amount and energy consumption of the charging node, respectively; while $\bar{D}_j^{\mathrm{trans}}$ and $\bar{E}_j^{\mathrm{trans}}$ are

the average transmitted data amount and energy consumption of the charging node, respectively.

C. The Solution Algorithm

It is evident from Fig. 3 that market clearing and pricing can be regarded as fixed-point problems, which can be solved using the iterative method presented in [41]. The iterative method comprises three sub-models, namely community network operator-optimization problem (CNO-OP), power distribution network-distribution locational marginal pricing (PDN-DLMP), and user equilibrium-convex model (UE-CVX). In this paper, the proposed sensitivity analysis can replace the UE-CVX sub-model, transforming the original bi-level model into a single-layer optimization problem. This simplification improves computational efficiency and allows the use of existing solvers to obtain solutions more quickly.

V. FR Control of BCSs in Real-time Market

This section introduces a real-time FR method for EVs, as illustrated in Fig. 3. The method leverages the calculated FRC in the intraday market. It incorporates a power-sharing mechanism for FR, which allocates AGC signals among BCSs based on the evaluated response coefficient.

A. Dynamic Response Coefficient Based FR Task Allocation

EVA allocates the FR task based on the response coefficient as follow:

$$P_j^{\mathrm{AGC,B}} = P^{\mathrm{AGC}} \times \frac{k_j^*}{\sum_{j\in J} k_j^*} \tag{11}$$

where $P_j^{\mathrm{AGC,B}}$ is the dispatched AGC task of BCS j; P^{AGC} is the dispatched AGC task of EVA from the power control center; and k_j^* is the evaluated response coefficient.

B. Dynamic Response Coefficient Evaluation Method

1) Influence Index Setting

The response characteristic index comprises FRC (Factor 1, F1), communication quality (F2), economic revenue deviation (F3). To obtain subjective-objective combined coefficients, the FAHP and CRITIC methods with the game theory are proposed. F1 aims to balance FRC utilization across BCSs and prevent FR task overload, F2 focuses on balancing the communication quality of BCSs, whereas F3 focuses on balancing the benefits by the difference between charging prices among BCSs.

2) Subjective Coefficient Evaluation Based on FAHP Method

The steps of using FAHP to evaluate subjective coefficients are as follows.

Step 1: Establish the evaluation matrix. Compare the importance of multiple indexes for BCS, and quantify their relative importance using the triangular fuzzy number scale, as shown in Table I, to construct a fuzzy evaluation matrix $\boldsymbol{A}'$:

$$\boldsymbol{A}' = (a'_{pq})_{3\times 3} = \begin{bmatrix} (1,1,1) & (l_{12},h_{12},u_{12}) & (l_{13},h_{13},u_{13}) \\ (l_{21},h_{21},u_{21}) & (1,1,1) & (l_{23},h_{23},u_{23}) \\ (l_{31},h_{31},u_{31}) & (l_{32},h_{32},u_{32}) & (1,1,1) \end{bmatrix} \tag{12}$$

where triangular fuzzy number $a'_{pq} = (l_{pq}, h_{pq}, u_{pq}) = (a'_{pq})^{-1} = (1/l_{pq}, 1/h_{pq}, 1/u_{pq})$; p and q denote the index number.

TABLE I
Triangular Fuzzy Number Scale

Hierarchy	Define	Triangular fuzzy number
1	Equally important	(1, 1, 1)
3	Slightly important	(2, 3, 4)
5	Quite important	(4, 5, 6)
7	Very important	(6, 7, 8)
9	Absolutely important	(9, 9, 9)

Step 2: Consistency test. Defuzzify the fuzzy evaluation matrix $\boldsymbol{D} = (d'_{pq})_{n\times n}$ by (13) and perform a consistency test on the obtained matrix. If the consistency ratio is less than or equal to 0.1, proceed; otherwise, reconstruct the fuzzy evaluation matrix.

$$d'_{pq} = \frac{l'_{pq} + h'_{pq} + u'_{pq}}{3} \tag{13}$$

Step 3: Calculate subjective coefficients. For triangular fuzzy numbers $M_1 = (l_1, h_1, u_1)$ and $M_2 = (l_2, h_2, u_2)$, the calculation rules are:

$$\begin{cases} M_1 \oplus M_2 = (l_1 + l_2, h_1 + h_2, u_1 + u_2) \\ M_1 \otimes M_2 = (l_1 l_2, h_1 h_2, u_1 u_2) \end{cases} \tag{14}$$

Calculate the geometric mean of the triangular fuzzy number set r'_p for each index and the fuzzy coefficient k'_p of each index by:

$$r'_p = \left(\prod_{q=1}^{n} a'_{pq} \right)^{1/n} \tag{15}$$

$$k'_p = r'_p \otimes (r'_1 \oplus r'_2 \oplus r'_3)^{-1} = (l_p, h_p, u_p) \tag{16}$$

Defuzzify and normalize to obtain the defuzzied subjective coefficients N_p of the indexes, as:

$$k_p = \frac{l_p + h_p + u_p}{3} \tag{17}$$

$$N_p = \frac{k_p}{\sum_{p=1}^{n} k_p} \tag{18}$$

Multiply the coefficients sequentially to obtain the subjective coefficients for the index layer, as:

$$\boldsymbol{K}^{\mathrm{s}}=(k_1^{\mathrm{s}},k_2^{\mathrm{s}},\cdots,k_n^{\mathrm{s}}) \tag{19}$$

3) Objective Coefficient Evaluation Based on the CRITIC

The CRITIC method is employed for objective coefficient evaluation. This approach captures the fluctuation and conflict among indexes. The process consists of the following steps.

Step 1: Construct and standardize the decision matrix with an initial decision matrix $\boldsymbol{X}$, which consists of four BCSs and three indexes, as:

$$\boldsymbol{X}=\begin{bmatrix} x_{11} & x_{12} & x_{13} \\ x_{21} & x_{22} & x_{23} \\ x_{31} & x_{32} & x_{33} \\ x_{41} & x_{42} & x_{43} \end{bmatrix} \tag{20}$$

where x_{jp} represents the pth factor for the jth BCS. The indices are classified into benefit index (higher is better) and cost index (lower is better). Their standardization are depicted as:

$$x_{jp}^{'}=\frac{x_{jp}-\min(x_p)}{\max(x_p)-\min(x_p)} \tag{21}$$

$$x_{jp}^{'}=\frac{\min(x_p)-x_{jp}}{\max(x_p)-\min(x_p)} \tag{22}$$

where $x_p=\{x_{1p},\ x_{2p},\ \cdots,\ x_{mp}\}$; and $x_{jp}^{'}$ denotes the standardized index. The standardized decision matrix $\boldsymbol{X}'$ is given as:

$$|\boldsymbol{X}'|=\begin{bmatrix} x_{11}^{'} & x_{12}^{'} & x_{13}^{'} \\ x_{21}^{'} & x_{22}^{'} & x_{23}^{'} \\ x_{31}^{'} & x_{32}^{'} & x_{33}^{'} \\ x_{41}^{'} & x_{42}^{'} & x_{43}^{'} \end{bmatrix} \tag{23}$$

Step 2: Calculate standard deviation and correlation coefficient. Measure volatility by calculating the standard deviation σ_p for each index and measure conflict r_{qp} by computing the correlation coefficient between indices, as:

$$\sigma_p=\sqrt{\frac{\sum_{p=1}^{m}(x_{pj}^{'}-\overline{x}_p)^2}{m}} \tag{24}$$

$$r_{qp}=\frac{\sum_{j=1}^{m}(x_{jq}^{'}-\overline{x}_q)(x_{jp}^{'}-\overline{x}_p)}{\sqrt{\sum_{j=1}^{m}(x_{jq}^{'}-\overline{x}_q)^2}\sqrt{\sum_{j=1}^{m}(x_{jp}^{'}-\overline{x}_p)^2}} \tag{25}$$

Step 3: Determine the information carrying capacity C_p of volatility and conflict. Combine standard deviation and correlation coefficient to define C_p of each index, as shown in (26). Indices with higher information carrying capacity are more important.

$$C_p=\sigma_p\sum_{p=1}^{n}(1-r_{qp}) \tag{26}$$

Step 4: Calculate objective coefficient vector:

$$\boldsymbol{K}^{\mathrm{o}}=(k_1^{\mathrm{o}},\ k_2^{\mathrm{o}},\ \cdots,\ k_m^{\mathrm{o}}) \tag{27}$$

$$k_p^{\mathrm{o}}=\frac{C_p}{\sum_{p=1}^{n}C_p}=\frac{\sigma_p\sum_{p=1}^{m}(1-r_{qp})}{\sum_{p=1}^{n}\left[\sigma_p\sum_{p=1}^{m}(1-r_{qp})\right]} \tag{28}$$

4) Combined Subjective and Objective Coefficient Based on Game Theory

In this section, game theory is applied to integrate the subjective and objective coefficients by minimizing deviations and achieving a Nash equilibrium for the comprehensive coefficient vector, thereby ensuring consistency between subjective and objective evaluations. The process follows these steps.

Step 1: Select a linear combination of the subjective $\boldsymbol{K}^{\mathrm{s}}$ and objective coefficient $\boldsymbol{K}^{\mathrm{o}}$ vectors of the indexes calculated in Section V.B.2) and Section V.B.3), as:

$$\boldsymbol{K}=\beta_1\boldsymbol{K}^{\mathrm{s}}+\beta_2\boldsymbol{K}^{\mathrm{o}},\ \ \beta_1,\beta_2>0 \tag{29}$$

where $\boldsymbol{K}$ is a vector of possible combination coefficients; β_1 and β_2 are linear combination coefficients.

Step 2: Construct an objective function using game theory to find the optimal linear combination of coefficients that minimizes the sum of $\boldsymbol{K}^{\mathrm{s}}$, $\boldsymbol{K}^{\mathrm{o}}$, and $\boldsymbol{K}$ deviations. The objective function is:

$$\min\left\|\boldsymbol{K}-\boldsymbol{K}^{\mathrm{s}}\right\|_2+\left\|\boldsymbol{K}-\boldsymbol{K}^{\mathrm{o}}\right\|_2 \tag{30}$$

Furthermore, based on the differential properties of the matrix, taking the first derivative of (30) results in:

$$\begin{bmatrix} \boldsymbol{K}^{\mathrm{s}}(\boldsymbol{K}^{\mathrm{s}})^{\mathrm{T}} & \boldsymbol{K}^{\mathrm{s}}(\boldsymbol{K}^{\mathrm{o}})^{\mathrm{T}} \\ \boldsymbol{K}^{\mathrm{o}}(\boldsymbol{K}^{\mathrm{s}})^{\mathrm{T}} & \boldsymbol{K}^{\mathrm{o}}(\boldsymbol{K}^{\mathrm{o}})^{\mathrm{T}} \end{bmatrix}\begin{bmatrix} \beta_1 \\ \beta_2 \end{bmatrix}=\begin{bmatrix} \boldsymbol{K}^{\mathrm{s}}(\boldsymbol{K}^{\mathrm{s}})^{\mathrm{T}} \\ \boldsymbol{K}^{\mathrm{o}}(\boldsymbol{K}^{\mathrm{o}})^{\mathrm{T}} \end{bmatrix} \tag{31}$$

Calculate the optimized linear combination coefficients β_1^* and β_2^*, and normalize it:

$$\begin{cases} \beta_1^*=\beta_1/(\beta_1+\beta_2) \\ \beta_2^*=\beta_2/(\beta_1+\beta_2) \end{cases} \tag{32}$$

Finally, a vector of combined subjective and objective coefficients of the adaptation evaluation indexes is obtained $\boldsymbol{K}^*=(k_1^*,\ k_2^*,\ \cdots,\ k_n^*)$:

$$\boldsymbol{K}^*=\beta_1^*\boldsymbol{K}^{\mathrm{s}}+\beta_2^*\boldsymbol{K}^{\mathrm{o}} \tag{33}$$

VI. Simulation Results

The simulation test system uses a modified IEEE33 DN and the Nguyen 16-point TN, as shown in Fig. 4. The TN parameters are detailed in Tables II [41], III and IV, with a base trip rate of 200 vehicles per hour.

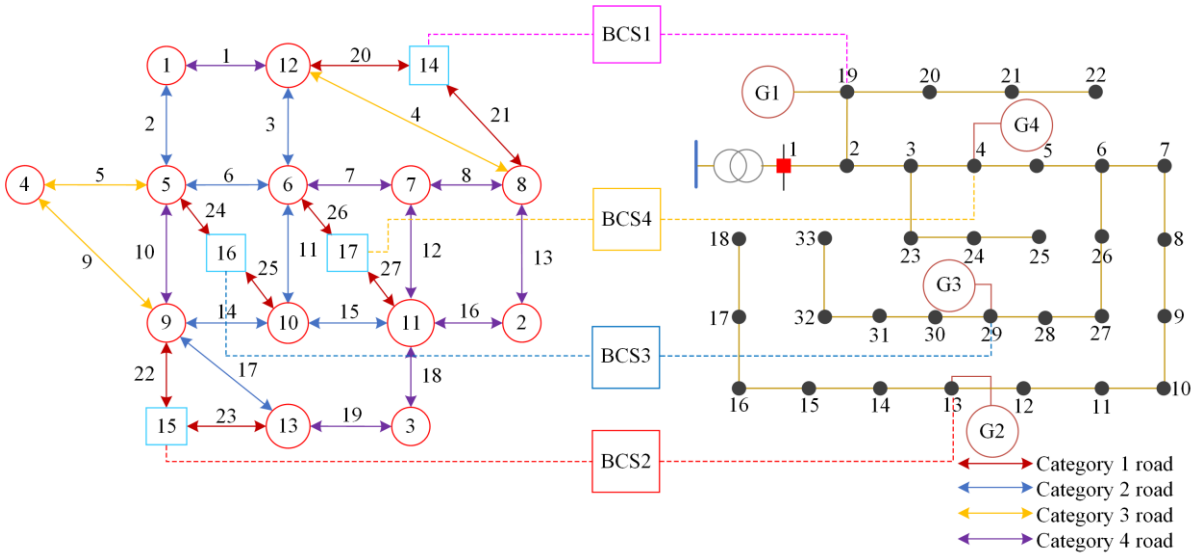

Fig. 4. Simulation system.

TABLE II
PARAMETERS OF THE SIMULATION MODEL

Parameters	Value	Parameters	Value
ω_0 ($/min)	0.5	c_a (p.u.)	60
R	0.9	c_ϕ (p.u.)	50
τ_c (hour)	0.4	t_a^{R0} (min)	20
E_D (kWh)	50	M_n (p.u.)	8
I_u (p.u.)	2	a_i ($/MW²·h)	0.24
b_i ($/MWh)	75	b_0 ($/MWh)	80
U^l (p.u.)	0.94	U^u (p.u.)	1.06
p_u^s (p.u.)	10	q_u^s (p.u.)	10
p_u^G (p.u.)	2.5	q_u^G (p.u.)	2.5
p_u^l (p.u.)	2.5	q_u^l (p.u.)	2.5

TABLE III
PARAMETER OF TRAFFIC DEMAND PAIRS

O-D pair	EV trip rate	GV trip rate
1→2	15	15
1→3	15	15
4→2	15	15
4→3	15	15

TABLE IV
PARAMETER OF TRAFFIC ROAD

Road category	Basic capacity	t_a^0
1	20	5
2	20	8
3	15	10
4	10	7

To validate the proposed method, 10 case studies (CSs) are designed. CS1: pricing method without considering road congestion alleviation [41]. CS2: proposed CPTS based pricing method considering road congestion alleviation. CS3: market clearing considering energy market profitability, excluding RC market participation [25]. CS4: combined economic dispatch and FR service for market clearing in both energy and RC markets. CS5: quantifying the load-price relationship using the demand self-elasticity model [42]. CS6: proposed load-price relationship quantitative methods using proposed sensitivity analysis. CS7: pricing method without sensitivity. CS8: proposed sensitivity-based pricing method for minimum electricity price change. CS9: power sharing for FR participation, only considering FRC balance [28]. CS10: proposed power sharing for FR participation, considering both FRC and benefit balance.

A. Verify the Price Method in Relieving Road Congestion and Balancing Communication Burden

To assess the effectiveness of the proposed pricing strategy in alleviating traffic congestion, a comparison between CS1 and CS2 is presented in Figs. 5 and 6. The optimized charging price is shown in Fig. 7, with a congestion rate threshold set at 0.8. In CS1, several roads, particularly roads 24 and 26, exceed the congestion threshold, due to their proximity to the BCS and their location along high-demand O-D paths. In contrast, the congestion rates in CS2 are significantly reduced, with most roads maintaining congestion rate below the 0.8. A more detailed analysis of the pricing strategy's impact on traffic flow is provided by the congestion rate at 16:00 in Fig. 8. The congestion rate of road 26 decreases to 0.767 p.u. as a result of the adjusted pricing. However, this reduction is offset by increased congestion on roads 20, 22, and 24. This shift occurs due to the higher charging price at BCS1, which is implemented to reduce traffic on road 26. In response, neighboring BCSs lowers their prices to attract more EVs, resulting in higher congestion on the surrounding roads. This shows how optimized charging prices interact with traffic flow and demonstrates the pricing strategy helps alleviate congestion in the TN.

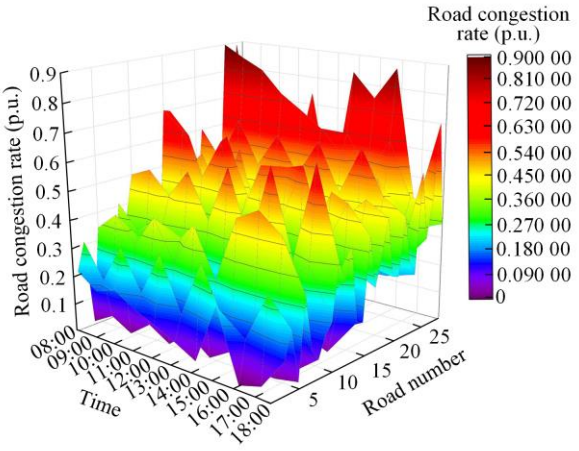

Fig. 5. Road congestion rate in CS1.

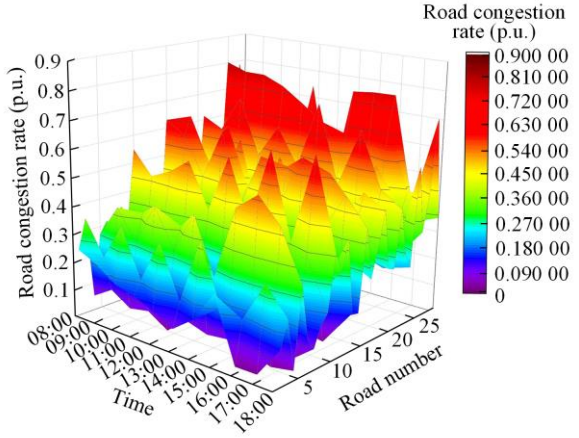

Fig. 6. Road congestion rate in CS2.

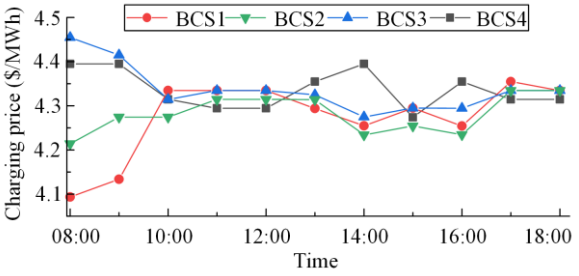

Fig. 7. Optimized charging price of BCSs.

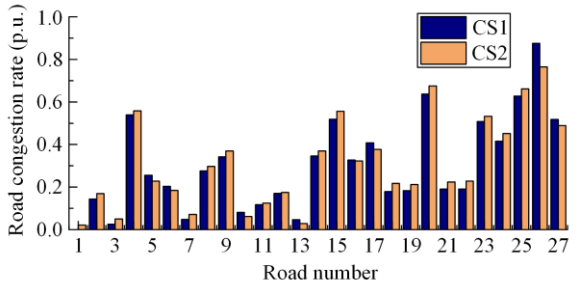

Fig. 8. Detailed road congestion rate.

Figure 9 depicts the price sensitivity of road congestion. For clarity, the horizontal axis represents the combination of BCS number and road reference value, while the vertical axis corresponds to road numbers. For instance, $(\mathrm{BCS4}(s_1),\ s_2)$ represents the sensitivity of BCS4 to roads $(s_1-1)\times 9+s_2$. The results reveal that congestion near BCSs exhibits strong positive correlation with price fluctuations, particularly for O-D paths connected to BCSs. Conversely, the sensitivity of non-adjacent roads is predominantly negative, consistent with findings in Fig. 7. Further validation of this sensitivity is provided in Section VI.C.

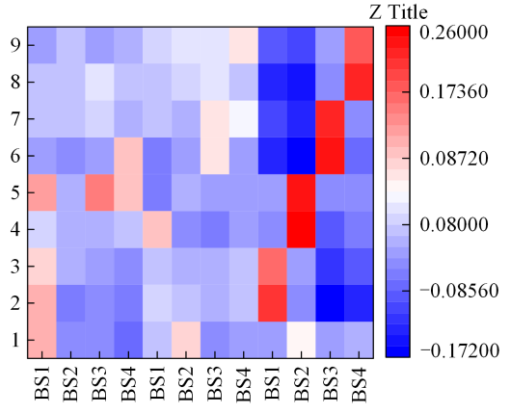

Fig. 9. Sensitivity of charging price to road congestion rate.

Figure 10 provides a detailed analysis of the communication quality of four BCSs at 16:00 in CS1 and CS2, specifically the data transmission volume and energy consumption of the charging nodes. Quantitative analysis reveals that CS2 demonstrates significantly reduced variance in both data throughput and energy utilization across its charging infrastructure compared to CS1. This indicates that CS2 can more effectively allocate and balance the communication load between BCS, thereby improving the overall system efficiency and stability.

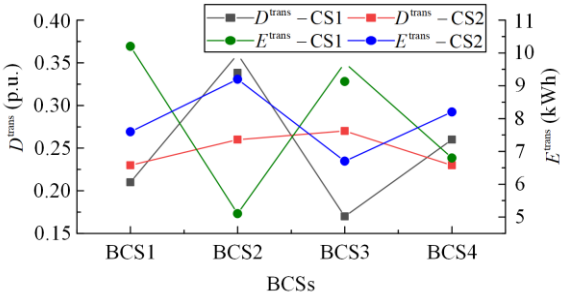

Fig. 10. Comparison of communication quality.

B. Verify the Pricing Method in Economic Benefit

To illustrate the economic advantages of the proposed pricing method, a comparison between CS3 and CS4 is conducted. As shown in Table V, CS4, which optimizes participation in both markets simultaneously, demonstrates superior profitability for BCSs compared to CS3. This is because CS3 focuses solely on minimizing energy costs by scheduling charging power, whereas CS4 leverages additional benefits from FRC participation in the RC market.

TABLE V
COMPARISON OF ECONOMIC PROFIT IN CS3 AND CS4

Profits	CS3	CS4
Energy profit	272.2	186.1
RC profit		476.6
Total profit	272.2	662.7

Figure 11 shows the charging and FRC schedules of BCS1 and BCS3 to explain the revenue difference. For example, at 12:00, when energy prices are low, CS3 reduces charging power to minimize costs. However, since the RC price at this time exceeds the energy price, CS4 not only reduces charging power but also adjusts FRC participation to maximize revenue.

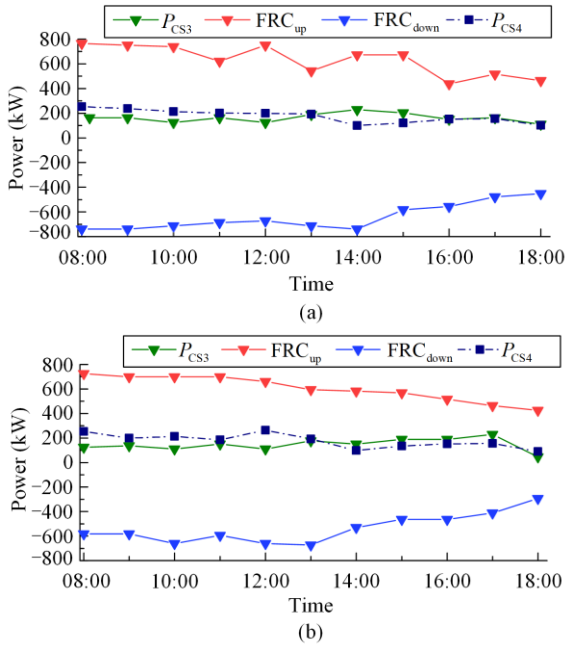

Fig. 11. Charging and FRC schedule. (a) BCS1. (b) BCS2.

C. Verify the Performance of Sensitivity Analysis

This section validates the accuracy of sensitivity analysis. A comparison of BCS revenues in CS5 and CS6 is conducted to evaluate the effectiveness of the demand elasticity and sensitivity models in predicting the impact of charging price changes on traffic congestion. This is particularly important for BCSs, as they incur penalty costs if the number of bids deviates from the actual charging schedule by more than 5%. Inaccurate predictions can also disrupt RC planning, negatively impacting overall BCS profitability.

Figures 12 and 13 present the profit and charging load of BCSs under CS5 and CS6, respectively. The sensitivity model outperforms the demand elasticity model in predicting EV traffic flow. This is because, in the demand elasticity model, the price of charging is seen as the directed variable for charging load. But the sensitivity model employs a BASS based meta-model, which identifies multiple influencing factors between price and traffic congestion, such as traffic constraints. These factors collectively affect EV charging decision, making the prediction results derived from the sensitivity analysis model closer to the actual traffic situation.

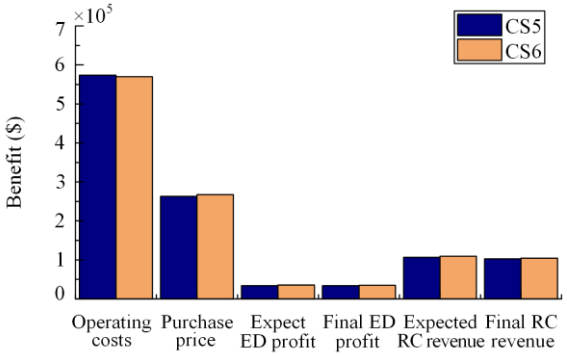

Fig. 12. Comparison of economic benefits.

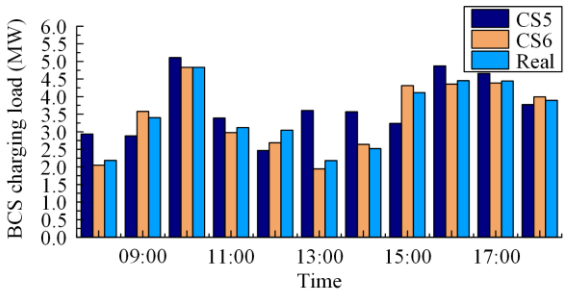

Fig. 13. Comparison of charging load estimation.

CS7 and CS8 further validate the advantages of sensitivity-based EV pricing. In a TN, sensitivity varies by traffic location, with higher sensitivity indicating that even minor price fluctuations can significantly impact traffic flow, thereby contributing to market stability for BCSs. Figure 14 depicts price changes for BCSs at 16:00 in response to congestion on road 26. It can be seen that there is a greater fluctuation in charging prices in CS7. Specifically, BCS3, which has lower sensitivity than BCS1 and BCS2, requires a substantial price reduction to divert traffic from BCS4. In contrast, BCS1 and BCS2, with higher sensitivity, achieve their objectives with only minor adjustments, resulting in more stable pricing.

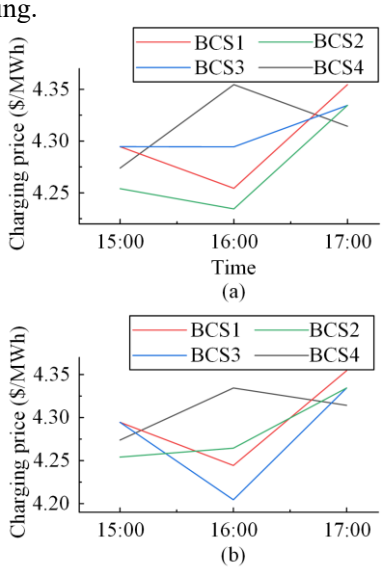

Fig. 14. Comparison of charging pricing. (a) CS7. (b) CS8.

D. Verify the Proposed FR Characteristic Assessment Method

CS9 and CS10 are compared to validate the performance of the proposed power sharing method for FR. First, the proposed method provides a subjective evaluation of the response characteristics of BCSs, described as:

$$\boldsymbol{A}' = (a'_{pq})_{3\times 3} = \begin{bmatrix} (1,\ 1,\ 1) & (3,\ 4,\ 5) & (7,\ 8,\ 9) \\ \left(\frac{1}{5},\ \frac{1}{4},\ \frac{1}{3}\right) & (1,\ 1,\ 1) & (3,\ 4,\ 5) \\ \left(\frac{1}{9},\ \frac{1}{8},\ \frac{1}{7}\right) & \left(\frac{1}{5},\ \frac{1}{4},\ \frac{1}{3}\right) & (1,\ 1,\ 1) \end{bmatrix} \tag{34}$$

Figure 15 presents the results of different objective coefficients, demonstrating that the CRITIC method effectively reduces volatility and conflicts within performance index data. The comprehensive coefficients for both objective and subjective indexes are calculated using game theory combinations that $\beta_1^* = 0.3325$, $\beta_2^* = 0.6675$, leading to the game linear combined coefficient for FR. As shown in Fig. 16, these combined coefficients incorporate both subjective decision-making experience and objective data factors. This mitigates the limitations of single evaluation methods while preserving the advantages of both subjective and objective assessments.

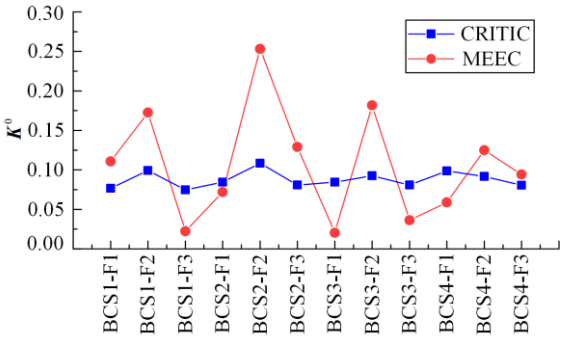

Fig. 15. Comparison of objective coefficients.

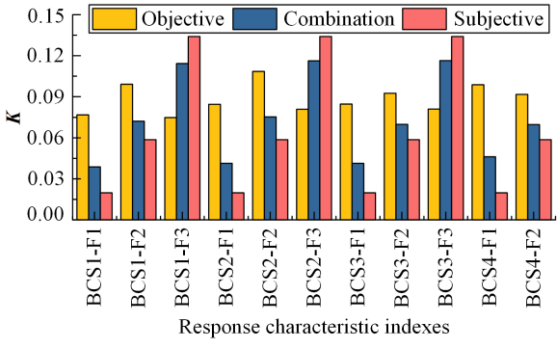

Fig. 16. Comparison of combined coefficients.

Figure 17 compares the effectiveness of FR between CS9 and CS10, revealing that both methods similarly suppress frequency fluctuations due to their balanced utilization of FRC. However, as indicated in Table VI, BCSs exhibit a greater advantage in terms of benefit balance.

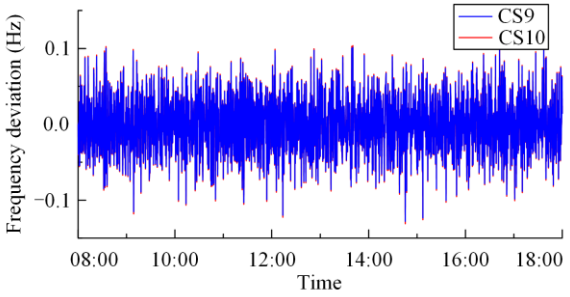

Fig. 17. Comparison of frequency deviation.

TABLE VI
COMPARISON OF THE BENEFIT IN REAL-TIME MARKET

BCSs revenue	CS3	CS4
BCS1 revenue	182.7	184.4
BCS2 revenue	181.8	184.7
BCS3 revenue	186.4	185.1
BCS4 revenue	188.9	185.4

VII. CONCLUSION

This paper presents a pricing and control method for multi-market operations, integrating the CPTS framework. In the intraday market, BCSs employ dynamic pricing to optimize traffic flow and alleviate congestion, while simultaneously coordinating the co-optimization of the energy and RC markets to maximize revenue. A novel subjective-objective evaluation facilitates effective collaboration between real-time and intraday markets, addressing the benefit imbalance among BCS under varying participation levels. Furthermore, the BASS-based sensitivity analysis for congestion-related pricing demonstrates high optimization accuracy with significantly reduced computational complexity. Simulation results validate the effectiveness of the proposed method in achieving optimal co-ordination between intraday and real-time markets, highlighting its potential to enhance BCS support capabilities within complex CPTS.

ACKNOWLEDGMENT

The authors would like to acknowledge the support of the Institute of Advanced Technology for Carbon Neutrality, Nanjing University of Posts and Telecommunications, Nanjing, China.

AUTHORS' CONTRIBUTIONS

Lei Xu: writing original draft, software, methodology, and conceptualization. Chunxia Dou: writing review, editing, and validation. Dong Yue: writing review, editing, and visualization. Houjun Li: supervision and data curation. Yanlin Ji: software. All authors read and approved the final manuscript.

FUNDING

This work is supported in part by the National Natural Science Foundation of China (No. 62293500 and No. 62293504) and in part by the Postgraduate Research and Practice Innovation Program of Jiangsu Province (No. KYCX23_1044).

AVAILABILITY OF DATA AND MATERIALS

Not applicable.

DECLARATIONS

Competing interests: The authors declare that they have no known competing financial interests or personal relationships that could have appeared to influence the work reported in this article.

AUTHORS' INFORMATION

Lei Xu is currently working toward the Ph.D. degree in information acquisition and control with the Nanjing University of Posts and Telecommunications, Nanjing, China. He is currently the vice dean of the research institute in the Jiangsu Off-Road Tyre Lifting Equipment Engineering and Technology Research Centre. His current research interests include modeling, operation, and control of virtual power plant, energy storage, and plug-in electric vehicles.

Chunxia Dou received the Ph.D. degree in control theory and control engineering from the Institute of Electrical Engineering, Yanshan University, Qinhuangdao, China, in 2005. In 2010, she joined the Department of Engineering, Peking University, Beijing, China, where she was a postdoctoral fellow for two years. Since 2015, she has been a professor with the Institute of Advanced Technology for Carbon Neutrality, Nanjing University of Posts and Telecommunications. Her current research interests include multi agent-based control, event-triggered hybrid control, distributed coordinated control, and multi-mode switching control and their applications in power systems, microgrids, and smart grids.

Dong Yue received the Ph.D. degree in control theory and control engineering from the South China University of Technology, Guangzhou, China, in 1995. He is currently a professor and the dean of the Institute of Advanced Technology for Carbon Neutrality and the director of the Academic Committee of the University, Nanjing University of Posts and Telecommunication. His current research interests include networked control, optimization, multi-agent systems, and smart grid. Dr. Yue was the recipient of the 2022 IEEE Rudolf Chope Research and Development Award, the Norbert Wiener Review Award by IEEE/CAA Journal of *Automatica Sinica* in 2020, and the Best Paper Award of IEEE Systems Journal in 2022. He was the chair of the IEEE IES Technical Committee on NCS and Applications. He was the co-editor-in-chief for *IEEE Transactions on Industrial Informatics* and the associate editor for *IEEE Industrial Electronics Magazine*, *IEEE Transactions on Systems*, *Man and Cybernetics: Systems*, *IEEE Transactions on Industrial Informatics*, *IEEE Transactions on Neural Networks and Learning Systems*, and *Journal of the Franklin Institute*.

Houjun Li received the B.S. degree from the College of Automation and Artificial Intelligence, Nanjing University of Posts and Telecommunications, Nanjing, China, in 2020, where he is currently working toward the Ph.D. degree in information acquisition and control with the Nanjing University of Posts and Telecommunications, Nanjing, China. His current research interests include graph Neural Networks, federated Learning, and the application of Artificial Intelligence in Power Systems.

Yanlin Ji is currently pursuing a Ph.D. in the Department of Engineering and Design at the University of Sussex, UK. He is also a member of the Advanced Communications Centre (ACMI) at Sussex. From June to September 2024, he was a visiting researcher at the School of Transportation Science and Engineering, Beihang University.

REFERENCES

[1] P. Sivalingam and M. Gurusamy, "Momentum search algorithm for analysis of fuel cell vehicle-to-grid system with large-scale buildings," *Protection and Control of Modern Power Systems*, vol. 9, no. 2, pp. 147-160, Mar. 2024.

[2] B. Xu, G. Zhang, and K. Li *et al*., "Reactive power optimization of a distribution network with high-penetration of wind and solar renewable energy and electric vehicles," *Protection and Control of Modern Power Systems*, vol. 7, no. 4, pp. 1-13, May 2022.

[3] S. Ahmed and M. H. Anisi, "Optimizing V2G dynamics: An AI-enhanced secure protocol for energy management in industrial cyber-physical systems," *IEEE Transactions on Industrial Cyber-Physical Systems*, vol. 2, pp. 312-320, Jul. 2024.

[4] S. Gao, H. Li, and J. Jurasz *et al*., "Optimal charging of electric vehicle aggregations participating in energy and ancillary service markets," *IEEE Journal of Emerging and Selected Topics in Industrial Electronics*, vol. 3, no. 2, pp. 270-278, Aug. 2022.

[5] Z. Zhou, S. J. Moura, and H. Zhang *et al*., "Power-traffic network equilibrium incorporating behavioral theory: a potential game perspective," *Applied Energy*, vol. 289, May 2021.

[6] A. Leippi, M. Fleschutz, and K. Davis *et al*., "Optimizing electric vehicle fleet integration in industrial demand response: maximizing vehicle-to-grid benefits while compensating vehicle owners for battery degradation," *Applied Energy*, vol. 374, Nov. 2024.

[7] S. Lü, G. Sun, and Z. Wei *et al*., "Optimal pricing and energy sharing of EV charging stations with an augmented user equilibrium model," *IEEE Transactions on Power Systems*, vol. 39, no. 2, pp. 4336-4349, Jun. 2023.

[8] C. Shao, K. Li, and T. Qian *et al*., "Generalized user equilibrium for coordination of coupled power-transportation network," *IEEE Transactions on Smart Grid*, vol. 14, no. 3, pp. 2140-2151, Sept. 2022.

[9] C. Shao, K. Li, and X. Li *et al*., "A decentralized bi-level decomposition method for optimal operation of electric vehicles in coupled urban transportation and power distribution systems," *IEEE Transactions on Transportation Electrification*, vol. 10, no. 1, pp. 2235-2246, Jun. 2023.

[10] M. Alizadeh, H.-T. Wai, and M. Chowdhury *et al*., "Optimal pricing to manage electric vehicles in coupled power and transportation networks," *IEEE Transactions on Control of Network Systems*, vol. 4, no. 4, pp. 863-875, Jul. 2016.

[11] S. Lü, S. Chen, and Z. Wei *et al*., "Power-transportation coordination: toward a hybrid economic-emission dispatch model," *IEEE Transactions on Power Systems*, vol. 37, no. 5, pp. 3969-3981, Nov. 2021.

[12] S. Lü, Z. Wei, and S. Chen *et al*., "Integrated demand response for congestion alleviation in coupled power and transportation networks," *Applied Energy*, vol. 283, Feb. 2021.

[13] T. N. Pham, A. M. T. Oo, and H. Trinh, "Event-triggered mechanism for multiple frequency services of electric vehicles in smart grids," *IEEE Transactions on Power Systems*, vol. 37, no. 2, pp. 967-981, Aug. 2022.

[14] I. A. Umoren, M. Z. Shakir, and H. Tabassum, "Resource efficient vehicle-to-grid (V2G) communication systems for electric vehicle enabled microgrids," *IEEE Transactions on Intelligent Transportation Systems*, vol. 22, no. 7, pp. 4171-4180, Sept. 2021.

[15] B. Zhou, K. Zhang and K. Chan *et al*., "Optimal coordination of electric vehicles for virtual power plants with dynamic communication spectrum allocation," *IEEE Transactions on Industrial Informatics*, vol. 17, no. 1, pp. 450-462, Apr. 2021.

[16] A. Orzechowski, L. Lugosch, and H. Shu *et al*., "A data-driven framework for medium-term electric vehicle charging demand forecasting," *Energy and AI*, vol. 14, Oct. 2023.

[17] L. Breiman, "Random forests," *Machine learning*, vol. 45, pp. 5-32, Oct. 2001.

[18] H. Kuang, H. Qu, and K. Deng *et al*., "A physics-informed graph learning approach for citywide electric vehicle charging demand prediction and pricing," *Applied Energy*, vol. 363, Jun. 2024.

[19] K. Ye, J. Zhao, and F. Ding *et al*., "Global sensitivity analysis of large distribution system with PVs using deep Gaussian process," *IEEE Transactions on Power Systems*, vol. 36, no. 5, pp. 4888-4891, May 2021.

[20] S. Gawusu and A. Ahmed, "Analyzing variability in urban energy poverty: a stochastic modeling and Monte Carlo simulation approach," *Energy*, vol. 304, Sept. 2024.

[21] J. N. Castillo, V. F. Resabala, and L. O. Freire *et al*., "Modeling and sensitivity analysis of the building energy consumption using the Monte Carlo method," *Energy Reports*, vol. 8, pp. 518-524, Dec. 2022.

[22] H. Zhang, W. Tian, and J. Tan *et al*., "Sensitivity analysis of multiple time-scale building energy using Bayesian adaptive spline surfaces," *Applied Energy*, vol. 363, Jun. 2024.

[23] D. Francom and B. Sanso, "Bass: an package for fitting and performing sensitivity analysis of Bayesian adaptive spline surfaces," *Journal of Statistical Software*, vol. 94, pp. 1-36, Sept. 2020.

[24] Y. Chen, S. Hu, and Y. Zheng *et al*., "Coordinated optimization of logistics scheduling and electricity dispatch for electric logistics vehicles considering uncertain electricity prices and renewable generation," *Applied Energy*, vol. 364, Jun. 2024.

[25] Q. Wang, C. Huang, and C. Wang *et al*., "Joint optimization of bidding and pricing strategy for electric vehicle aggregator considering multi-agent interactions," *Applied Energy*, vol. 360, Apr. 2024.

[26] D. Qiu, Z. Dong, and G. Ruan *et al*., "Strategic retail pricing and demand bidding of retailers in electricity market: a data-driven chance constrained programming," Advances in *Applied Energy*, vol. 7, Sept. 2022.

[27] G. S. Pavlak, G. P. Henze, and V. J. Cushing, "Optimizing commercial building participation in energy and ancillary service markets," *Energy and Buildings*, vol. 81, pp. 115-126, Oct. 2014.

[28] S. Gao, R. Dai, and W. Cao *et al*., "Combined provision of economic dispatch and frequency regulation by aggregated EVs considering electricity market interaction," *IEEE Transactions on Transportation Electrification*, vol. 9, no. 1, pp. 1723-1735, Mar. 2022.

[29] S. Gao, H. Li, and J. Jurasz *et al*., "Optimal charging of electric vehicle aggregations participating in energy and ancillary service markets," *IEEE Journal of Emerging and Selected Topics in Industrial Electronics*, vol. 3, no. 2, pp. 270-278, Apr. 2021.

[30] B. Vatandoust, A. Ahmadian, and M. A. Golkar *et al*., "Risk-averse optimal bidding of electric vehicles and energy storage aggregator in day-ahead frequency regulation market," *IEEE Transactions on Power systems*, vol. 34, no. 3, pp. 2036-2047, May 2018.

[31] Y. Li, M. Han, and Z. Yang *et al*., "Coordinating flexible demand response and renewable uncertainties for scheduling of community integrated energy systems with an electric vehicle charging station: a bi-level approach," *IEEE Transactions on Sustainable Energy*, vol. 12, no. 4, pp. 2321-2331, Oct. 2021.

[32] H. Liu, J. Qi, and J. Wang *et al*., "EV dispatch control for supplementary frequency regulation considering the expectation of EV owners," *IEEE Transactions on Smart Grid*, vol. 9, no. 4, pp. 3763-3772, Jul. 2016.

[33] H. Liu, Z. Hu, and Y. Song *et al*., "Vehicle to-grid con-

trol for supplementary frequency regulation considering charging demands," *IEEE Transactions on Power Systems*, vol. 30, no. 6, pp. 3110-3119, Nov. 2015.

[34] M. Wang, Y. Mu, and Q. Shi *et al*., "Electric vehicle aggregator modeling and control for frequency regulation considering progressive state recovery," *IEEE Transactions on Smart Grid*, vol. 11, no. 5, pp. 4176-4189, Sept. 2020.

[35] S. Kiani, K. Sheshyekani, and H. Dagdougui, "An extended state space model for aggregation of large-scale EVs considering fast charging," *IEEE Transactions on Transportation Electrification*, vol. 9, no. 1, pp. 1238-1251, Mar. 2022.

[36] K. Kaur, N. Kumar, and M. Singh, "Coordinated power control of electric vehicles for grid frequency support: Milp-based hierarchical control design," *IEEE Transactions on Smart Grid*, vol. 10, no. 3, pp. 3364-3373, May 2018.

[37] L. Wang, S. Sharkh, and A. Chipperfield *et al*., "Dispatch of vehicle-to-grid battery storage using an analytic hierarchy process," *IEEE Transactions on Vehicular Technology*, vol. 66, no. 4, pp. 2952-2965, Apr. 2017.

[38] J. Deng, B.Chen, and J. Lu *et al*., "Thermal runaway and combustion characteristics, risk and hazard evaluation of lithium-iron phosphate battery under different thermal runaway triggering modes," *Applied Energy*, vol. 368, Aug. 2024.

[39] Y. Zhang and K. Shang, "Evaluation of mine ecological environment based on fuzzy hierarchical analysis and grey relational degree," *Environmental Research*, vol. 257, Sept. 2024.

[40] C. Zhang, J. Xia, and X. Guo *et al*., "Multi-optimal design and dispatch for a grid-connected solar photovoltaic-based multigeneration energy system through economic, energy and environmental assessment," *Solar Energy*, vol. 243, pp. 393-409, Sept. 2022.

[41] Y. Cui, Z. Hu, and X. Duan, "Optimal pricing of public electric vehicle charging stations considering operations of coupled transportation and power systems," *IEEE Transactions on Smart Grid*, vol. 12, no. 4, pp. 3278-3288, Jul. 2021.

[42] N. G. Paterakis, A. Tascıkaraoglu, and O. Erdinc *et al*., "Assessment of demand-response-driven load pattern elasticity using a combined approach for smart households," *IEEE Transactions on Industrial Informatics*, vol. 12, no. 4, pp. 1529-1539, Aug. 2016.